Cross-Influence of Temperature and Front Layer Thickness on the Performance of a Heterojunction Solar Cell

Abstract

This study investigates the combined influence of temperature and the thickness of the front surface field (FSF) layer on the electrical performance of a heterojunction solar cell with the structure [(p^+)-a-Si:H/(n)-c-Si/(n^+)-a-Si:H]. The analysis is based on numerical simulations performed using the Atlas module of the TCAD SILVACO suite, considering a temperature range from 275 K to 330 K and FSF layer thicknesses varying between 2 nm and 20 nm.

The simulation results reveal a simultaneous degradation of both the open-circuit voltage (V_{oc}) and the short-circuit current density (J_{sc}) as the temperature increases, particularly in the intermediate FSF thickness range of 3–10 nm. This behavior is primarily attributed to the enhanced carrier recombination at elevated temperatures, especially when the FSF layer is too thin to ensure effective field-induced passivation.

In contrast, thicker FSF layers, specifically those ranging from 13 nm to 20 nm, exhibit improved thermal stability and reduced sensitivity to temperature-induced performance losses. This improvement is likely due to better electric field formation and interface passivation, which mitigate recombination at the a-Si:H/c-Si junction. On the other hand, ultrathin FSF layers (< 5 nm) result in insufficient band bending and weak field-effect passivation, thereby increasing interface recombination and significantly degrading the photovoltaic efficiency.

Overall, the findings underscore the critical role of FSF layer thickness in determining the thermal and optoelectronic behavior of heterojunction solar cells. They highlight the need for simultaneous optimization of the FSF thickness and the cell's thermal operating conditions to ensure stable and efficient performance under realistic environmental variations.

Keywords: solar cell, heterojunction, silicon, amorphous silicon, FSF, thickness, temperature, simulation, TCAD-SILVACO

1. Introduction

Silicon-based heterojunction (HJT – Heterojunction with Intrinsic Thin layer) photovoltaic (PV) solar cells represent a highly promising architecture due to their high efficiency and excellent passivation properties. This stable technology integrates two types of semiconductor materials, typically arranged in a trilayer structure forming dual p-n junctions: hydrogenated amorphous silicon / crystalline silicon / hydrogenated amorphous silicon (p^+-a-Si:H / n-c-Si / n^+-a-Si:H). The ability to combine amorphous and crystalline silicon within a single PV device has attracted significant attention over the past decades and has been the subject of extensive research efforts **[1, 2]**.

In this study, we present simulation results focusing on key performance indicators such as the short-circuit current density (J_{sc}), the open-circuit voltage (V_{oc}), the fill factor (FF), and the conversion efficiency (η) for an HJT solar cell (p^+-a-Si:H / n-c-Si / n^+-a-Si:H). The simulations are carried out using the ATLAS module of the TCAD-SILVACO software suite **[3]**, with a particular emphasis on the influence of temperature variations and the optimization of the front surface field (FSF) layer.

2. Electrical Modeling of a Solar Cell

A photovoltaic solar cell can be modeled by an equivalent electrical circuit consisting of a current source that represents the incident light power, a diode accounting for the polarization phenomena, a series resistance representing various contact and interconnection resistances, and a parallel (shunt) resistance characterizing leakage currents caused by the diode and edge effects at the p–n junction of the solar cell. The equivalent circuit diagram is shown in Figure 1.

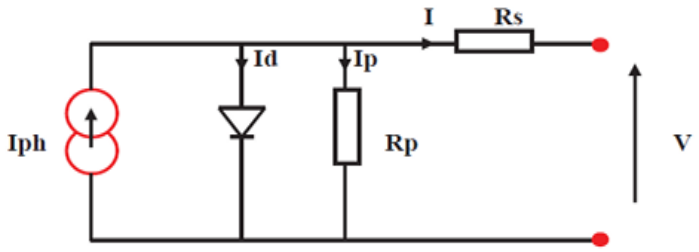

Figure 1 : Equivalent Circuit of a Photovoltaic Solar Cell

Based on the operating principles of photovoltaic (PV) solar cells and their current–voltage (I–V) characteristics under illumination, the evaluation of their electrical performance relies on several key quantities known as photovoltaic parameters **[3,4]**. The most relevant among them include the fill factor (FF), open-circuit voltage (V_{oc}), short-circuit current density (J_{sc}), and power conversion efficiency (η).

- Short-Circuit Current (I_{sc})

The short-circuit current represents the maximum current delivered by a PV solar cell when the terminal voltage is zero. It is a critical parameter for the characterization of photovoltaic devices. This current is directly proportional to the intensity of the incident light.

Under illumination, the output current at the terminals of the p–n junction constituting the solar cell is given by the following expression **[6,7]**:

The current–voltage relationship of a photovoltaic solar cell can be described by the following expression:

$$I_L = I_{ph} - I_D - I_{sh} = I_{ph} - I_0\left[\exp\left(\frac{q(V + I_L R_S)}{nkT}\right) - 1\right] - \frac{V + I_L R_S}{R_{sh}} \quad (1)$$

Where:

- k is the Boltzmann constant,
- T is the absolute temperature,
- q is the elementary charge,
- I_{ph} is the photocurrent, approximately equal to I_{sc},
- I_0 is the dark saturation current,
- I_D is the diode current,
- I_{sh} is the shunt current,
- V is the output voltage,
- n is the ideality factor, typically between 1 and 2,
- R_S and R_{Sh} are the series and shunt resistances, respectively.

The photocurrent I_{ph} depends on both irradiance and temperature and is expressed as **[8, 9]**:

$$I_{ph} = \left(I_{ph_{ref}} + \alpha(T - T_{ref})\right).\frac{G}{G_{ref}} \quad (2)$$

The saturation current I_0 is given by:

$$I_0 = I_{rs}\left[\frac{T}{T_{ref}}\right]^3 \exp\left[\frac{qE_g}{nkT}\left(\frac{T}{T_{ref}}\right)\right] \quad (3)$$

With:

$$I_0 = I_{rs}\left[\frac{T}{T_{ref}}\right]^3 \exp\left[\frac{qE_g}{nkT}\left(\frac{T}{T_{ref}}\right)\right] \quad (3)$$

$$I_{rs} = \frac{I_{ph}}{\left[\exp\left(\frac{qV_{oc}}{nkT}\right) - 1\right]} \quad (4)$$

Where I_{rs} is the diode reverse saturation current.

- Open-Circuit Voltage (V_{oc})

The open-circuit voltage, denoted V_{oc}, is the voltage measured across the terminals of a solar cell when the output current is zero ($I = 0$), i.e., when the cell is connected to an infinite load resistance. This parameter depends on several factors, including the type of solar cell, the materials used in the active layer, the nature of the contact between the active layer and the electrodes, and the illumination conditions **[5]**.

It is given by the following equation:

$$V_{oc} = \frac{nkT}{q}.\ln\left(\frac{I_{ph}}{I_0} + 1\right) \quad (6)$$

The open-circuit voltage V_{oc} is proportional to the contact potential difference V_D, defined as:

$$V_D = \frac{kT}{q}\ln\left(\frac{N_D.N_A}{n_i^2}\right) \quad (7)$$

where the intrinsic carrier concentration n_i is expressed as:

$$n_i = AT^{3/2}\exp\left(-\frac{E_g}{2kT}\right) \quad (8)$$

with:

- N_D: donor atom concentration,
- N_A acceptor atom concentration,
- n_i: intrinsic carrier concentration,
- E_g: bandgap energy,
- A: a constant specific to the semiconductor.

In Equation (8), the exponential term $\exp\left(-\frac{E_g}{2kT}\right)$ dominates over the polynomial dependence $T^{3/2}$, allowing the variation of n_i with temperature to be considered essentially exponential.
As the temperature *T* increases, the intrinsic carrier concentration n_i also increases, leading to a decrease in V_D according to Equation (7), and consequently a reduction in V_{oc}.

- Electrical Power (P)

Under standard environmental conditions (illumination, temperature, etc.), the electrical power P (in watts) delivered by a photovoltaic cell is defined as the product of the direct current I supplied by the cell and the output voltage V **[10, 11]**:

$$P(W) : U * I$$

- **P (W)**: Electrical power measured at the terminals of the PV solar cell.
- **U (V)**: Voltage measured across the cell.
- **I (A)**: Current delivered by the cell.

- Fill Factor (FF)

The fill factor is a dimensionless parameter used to evaluate the quality of a photovoltaic solar cell. It quantifies the ratio between the maximum power output of the cell and the theoretical power defined by the product of the open-circuit voltage and the short-circuit current. It is expressed as:

- $FF = \frac{P_{max}}{V_{oc} . I_{cc}}$ (9)
- P_{max} (W): Maximum power delivered by the cell, corresponding to the operating point (V_{max}, I_{max}):

$$P_{max} = V_{max} * I_{max}$$

- V_{max} : Voltage at the maximum power point.
- I_{max} : Current at the maximum power point.
- V_{oc} (V): Open-circuit voltage.
- I_{cc} (A): Short-circuit current.

The fill factor depends on several factors, including cell design, the quality of the p–n junction, the semiconductor material, and the resistivity of the metallic contacts.

- Conversion Efficiency (η)

The conversion efficiency of a photovoltaic cell is the ratio of the maximum electrical power P_{max} to the incident optical power. It can be improved by increasing the fill factor, the short-circuit current, and the open-circuit voltage. The efficiency is defined as:

$$\eta = \frac{P_{max}}{P_{inc} . S} = \frac{V_{max} . I_{max}}{P_{inc} . S} = FF . \frac{V_{oc} . I_{cc}}{P_{inc} . S} \quad (10)$$

where P_{inc} is the incident power per unit area and S is the surface area of the cell.

3. Matériels, méthodes and Simulation Parameters

The heterojunction solar cell (HJT) is a photovoltaic technology that combines two types of semiconductors. Its structure consists of three layers: a crystalline silicon (c-Si) layer acting as the active region, sandwiched between two heavily doped hydrogenated amorphous silicon (a-Si:H) layers. The front and rear layers serve as the front surface field (FSF) and back surface field (BSF), respectively. This multilayer configuration (p^+)-a-Si:H / (n)-c-Si / (n^+)-a-Si:H enhances light absorption and improves overall energy conversion efficiency.
In this work, we investigate the effect of temperature variation on the electrical performance of the HJT solar device. The study is carried out using the Atlas simulator from the TCAD SILVACO software suite **[3]**. This 2D/3D device simulator enables predictive modeling of the electrical

characteristics of semiconductor components. In addition to external electrical parameters, it provides access to internal variables such as electric field distribution and potential profiles.

These results are obtained by numerically solving Poisson's equation along with the continuity equations for electrons and holes over a discretized mesh representing the device structure. Carrier recombination mechanisms including Auger and Shockley-Read-Hall (SRH) are also taken into account, depending on the doping profile. A schematic representation of a typical HJT cell architecture is provided in **Figure 2**.

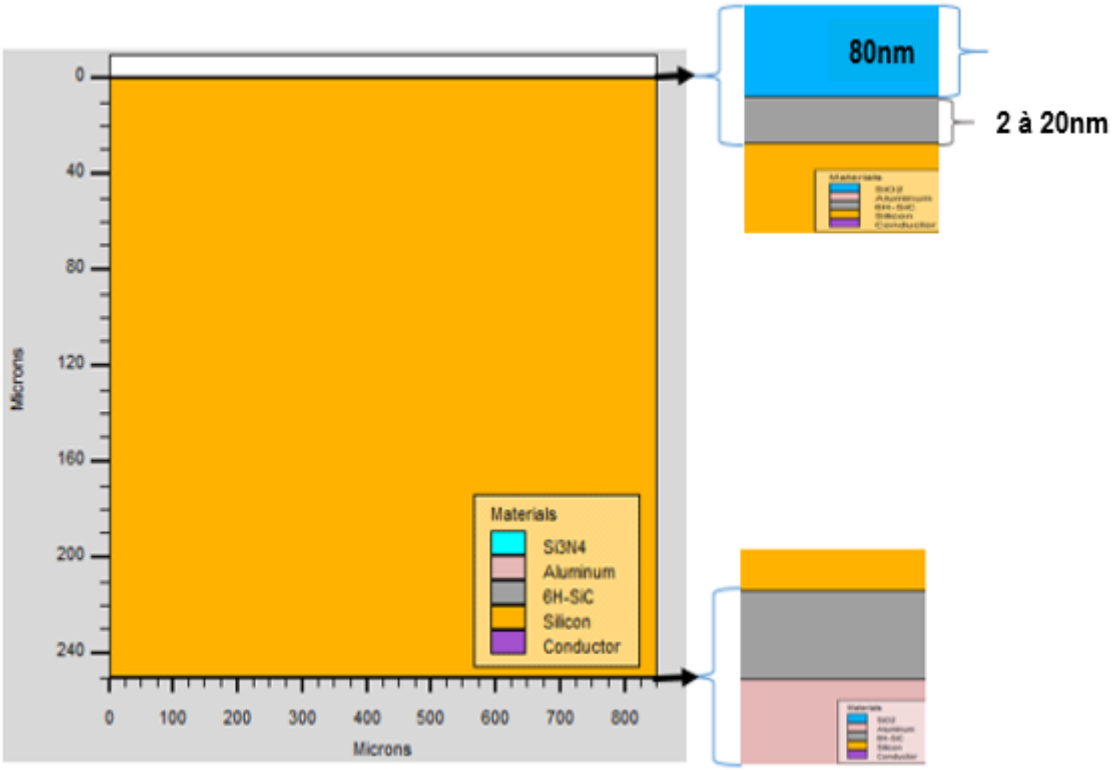

Figure 2 : Schematic Structure of the Heterojunction PV Solar Cell to Be Simulated

Simulating the photovoltaic solar cell structure with **TCAD-SILVACO** requires inputting the physical parameters of each material layer composing the device.

Table 1: Physical properties of materials used in the simulation

Different Layers / Physical properties	FSF (a-Si:H)	BSF (a-Si:H)	Substrate (c-Si)	Units
Thickness	0.1	0.1	250	μ_m
$\mathbf{E_g}$	1.7	0.7	1.12	eV
$\boldsymbol{\chi}$	3.9	3.9	4.05	eV
$\boldsymbol{\mu_n}$	1.10^{-6}	1.10^{-6}	1.10^{-3}	$cm^{-2}/V.s$
$\boldsymbol{\mu_p}$	1.10^{-6}	1.10^{-6}	1.10^{-3}	$cm^{-2}/V.s$
$\mathbf{N_c}$	2.10^{20}	2.10^{20}	$2.8\ 10^{19}$	cm^{-3}
$\mathbf{N_v}$	2.10^{20}	2.10^{20}	$1.04\ 10^{19}$	cm^{-3}
$\boldsymbol{\varepsilon}$	11.9	11.9	11.9	F/cm

E_g : energy bandgap

χ : electron affinity

μ_n, μ_p : electron and hole mobilities

N_c, N_v : effective density of states in the conduction and valence bands

ε : relative permittivity

The defect states present in the thin hydrogenated amorphous silicon layers (notably in the BSF, and variably in the FSF) are characterized by the parameters listed in the following table.

Table 1 : Simulation parameters for defect state densities and capture cross-sections

Defect parameters	**Acceptor defects (A)**	**Donor defects (D)**	**Units**
$\mathbf{N_{GA}, N_{GD}}$	$1{,}5.10^{15}$	$1{,}5.10^{15}$	cm^{-3}
$\mathbf{N_{TA}, N_{TD}}$	1.10^{21}	1.10^{21}	cm^{-3}
$\mathbf{E_{GA}, E_{GD}}$	0,62	0.78	eV
$\mathbf{W_{GA}, W_{GD}}$	0,15	0.15	eV
$\mathbf{W_{TA}, W_{TD}}$	0.033	0.049	eV
$\boldsymbol{\sigma_n}$	1.10^{-17}	1.10^{-15}	cm^{-2}
$\boldsymbol{\sigma_P}$	1.10^{-15}	1.10^{-17}	cm^{-2}

N_{GA}, N_{GD} : Gaussian-shaped acceptor/donor defect densities

N_{TA}, N_{TD} : Tail state densities near the conduction/valence bands

E_{GA}, E_{GD} : Energy position of the Gaussian peak

W_{GA}, W_{GD} : Width of the defect energy distribution

W_{TA}, W_{TD} : Largeur de la distribution

σ_n, σ_P : Electron and hole capture cross-sections

All simulations were conducted under standard test conditions: AM1.5 spectrum, 0.1 W/cm² irradiance, and a temperature of 300 K.

4. Results and Discussion

Photovoltaic solar cells are optoelectronic devices capable of converting solar energy directly into electrical energy. Designed for outdoor use, these cells are exposed to significant temperature variations, ranging from early morning cold to peak sunlight heat, depending on their location. Therefore, understanding their electrical behavior across a wide temperature range is essential.

In this study, we examine the effect of temperature variation (from 275 K to 330 K) on the main electrical performance parameters of a heterojunction solar cell, including voltage, power, current density, fill factor, and efficiency. The analysis is performed using the Atlas simulator from the TCAD-SILVACO software suite.

4.1. Temperature Effect on Conversion Efficiency (η).

Figure 3 illustrates the variation in conversion efficiency of the heterojunction solar cell as a function of temperature, for different thicknesses of the FSF layer.

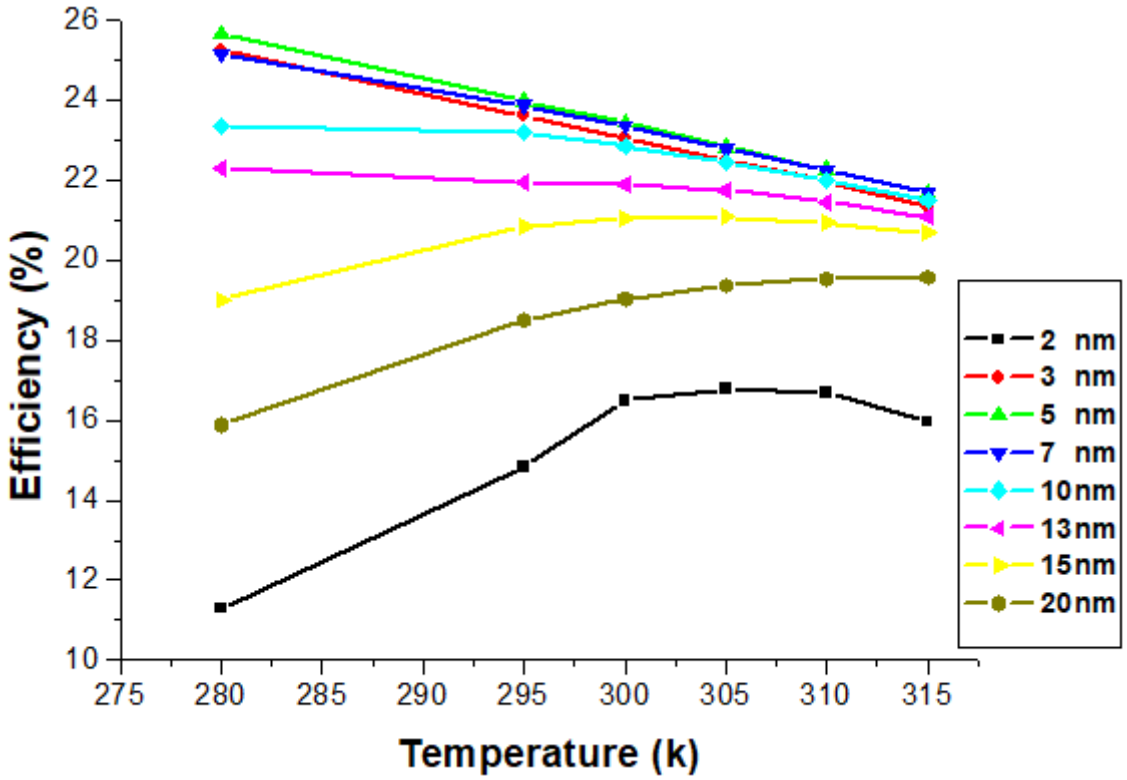

Figure 3 : Efficiency Evolution of a Cell with Varying FSF Layer Thicknesses as a Function of Temperature

Simulation results show that for photovoltaic solar cells with FSF layer thicknesses ranging from 3 nm to 10 nm, the conversion efficiency (η) exhibits a significant decline as the temperature increases from 275 K to 330 K. In contrast, for FSF thicknesses between 13 nm and 15 nm, the efficiency improves steadily with temperature up to 300 K, followed by a slight decrease or stabilization. A specific trend is also observed for cells with 2 nm and 20 nm thick FSF layers, which show a slight increase in efficiency within the same temperature range.

The pronounced efficiency drop in the 3–10 nm range can be attributed to the enhanced thermal agitation of free charge carriers, leading to a reduction in diffusion length and an increase in non-radiative recombination rates. Thin FSF layers are more prone to localized thermal accumulation, which limits charge collection and reduces performance at elevated temperatures **[12]**.

Conversely, the improvement in efficiency observed for the 20 nm FSF layer is explained by a longer diffusion length that benefits from thermal activation. In this case, carriers that previously struggled to traverse the space-charge region due to insufficient diffusion are assisted by thermal energy, resulting in improved separation and collection that partially compensates for recombination losses.

The efficiency curve also highlights a significant performance drop when the front a-Si:H layer is reduced to an ultrathin thickness of 2 nm. Contrary to explanations based on excessive optical transparency, this drop is more accurately attributed to poor passivation of the crystalline silicon surface. As demonstrated by Bivour et al. (2012) **[13]**, when the a-Si:H layer thickness falls below 5 nm, the passivation quality at the a-Si:H/c-Si interface degrades significantly, leading to increased surface recombination and reduced efficiency.

This observation is supported by Taguchi et al. (1994) **[14]**, who showed that optimal passivation using a-Si:H is a critical factor for achieving high-efficiency heterojunction cells. The deposition of an

ultrathin front layer compromises both junction formation and surface passivation, leading to a sharp increase in recombination losses.

An optimized front layer thickness thus provides a necessary balance between effective electronic passivation and sufficient optical transparency, ensuring efficient photocarrier collection and enhanced photovoltaic performance.

In addition, the efficiency curve reveals a progressive improvement in cell performance between 270 K and 300 K, followed by a plateau. This behavior may be attributed to increased thermal agitation, which facilitates the release of charge carriers trapped in shallow energy states, temporarily reducing recombination losses and enhancing the overall conversion efficiency.

4.2.Effect of Temperature on the Short-Circuit Current Density (J_{sc})

The current density generated by a solar cell results from the sum of the diffusion current densities of electrons and holes, along with the dominant generation current in the depletion region. It can be expressed by the following relation:

$$J = J_P + J_S = J_S\left[\exp\left(\frac{qV}{KT}\right) - 1\right] = \left(\frac{qD_p p_{n0}}{L_p} + \frac{qD_n n_{p0}}{L_n}\right)\left[\exp\left(\frac{qV}{KT} - 1\right)\right] \quad (11)$$

where:

- J_S is the saturation current density,
- D_n and D_p are the diffusion coefficients of electrons and holes, respectively,
- $L_n = \sqrt{D_n \tau}$ and $L_p = \sqrt{D_p \tau}$ are the corresponding diffusion lengths,
- n_{p0} and p_{n0} represent the minority carrier concentrations in the p-type and n-type regions,

This equation clearly shows that the current density is inversely affected by temperature. As temperature increases, the thermal agitation of charge carriers intensifies, which disrupts carrier transport and reduces their collection efficiency—ultimately leading to a decrease in short-circuit current density.

Figure 4 illustrates the evolution of the current density in a heterojunction solar cell as a function of temperature, for various FSF layer thicknesses.

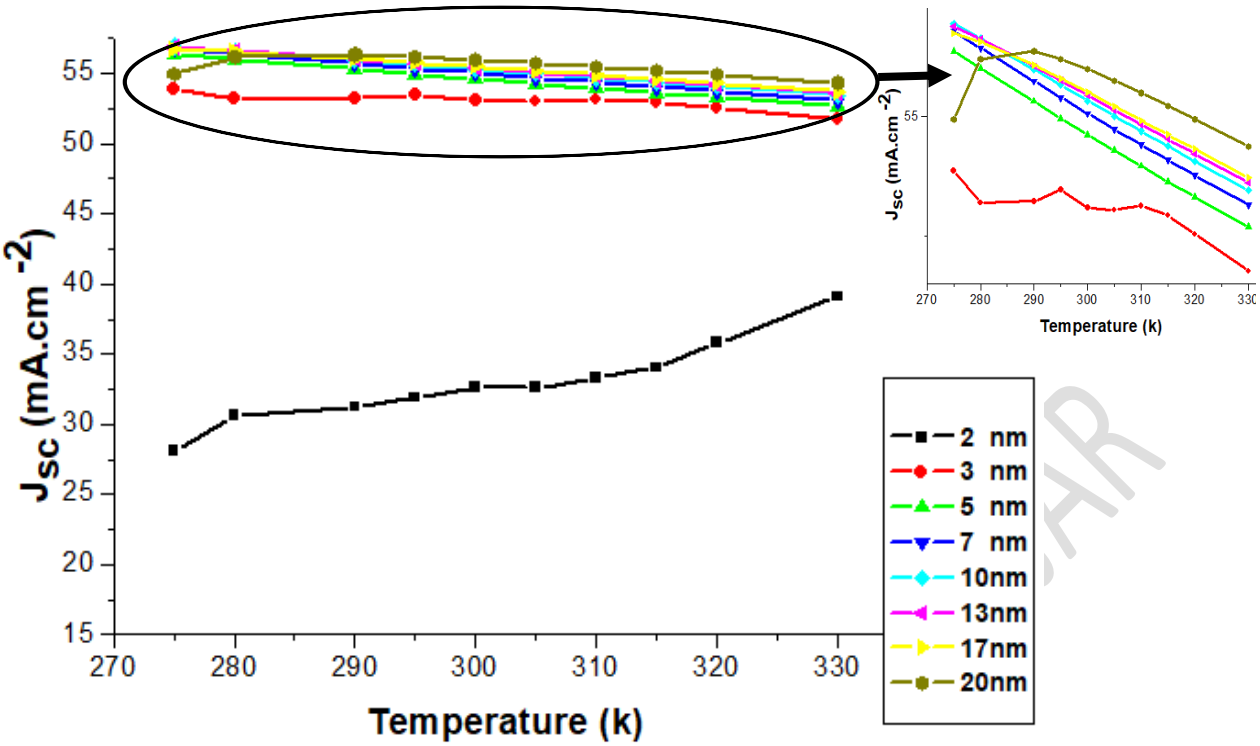

Figure 4 : Evolution of Current Density as a Function of Temperature for Various FSF Layer Thicknesses

The results presented in Figure 4 reveal a quasi-linear decrease in current density as the temperature increases. This trend is consistent with the theoretical expression that relates current density, voltage, and temperature, as established in **(11)**.

Furthermore, the observed variation strongly depends on the thickness of the emitter layer (FSF). For thicknesses between 5 nm and 20 nm, the current density decreases in a gradual and relatively uniform manner with temperature. In contrast, for a cell with an FSF layer of 3 nm, the current density remains almost constant, despite the rise in temperature indicating apparent thermal stability for this configuration.

However, when the FSF thickness drops below 3 nm, a noticeable performance degradation is observed. This is attributed to a significant deterioration in the passivation quality of the a-Si:H / c-Si interface, which leads to increased non-radiative recombination. As a result, the current density decreases due to less efficient collection of photogenerated carriers.

Effect of Temperature on the Fill Factor (FF)

Figure 5 illustrates the variation of the fill factor (FF) of a heterojunction solar cell as a function of temperature, for different FSF layer thicknesses. This analysis provides insight into how temperature affects the quality of the maximum power point, and therefore the overall performance of the device.

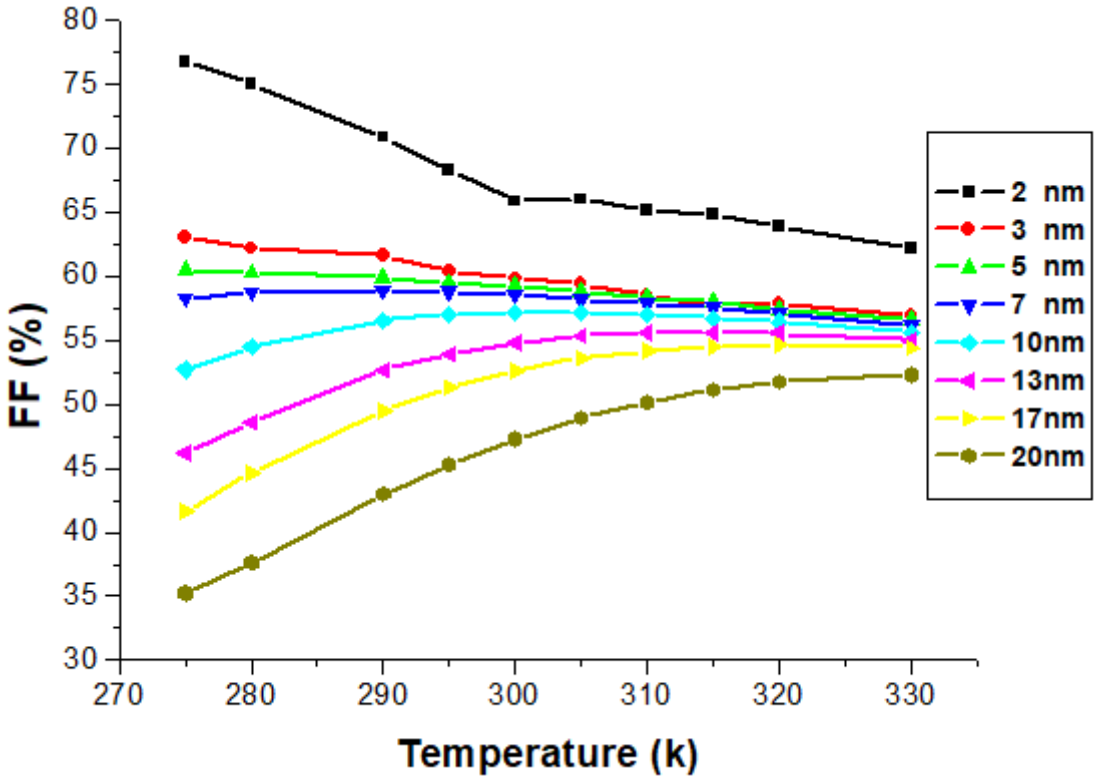

Figure 5 : Evolution of the Fill Factor of a Photovoltaic Cell as a Function of Temperature for Different FSF Layer Thicknesses

The analysis of Figure 5 reveals distinct trends in the evolution of the fill factor (FF) with temperature, depending on the FSF layer thickness:

- A decrease in FF is observed for photovoltaic cells with FSF thicknesses of 3 nm and 5 nm;
- A stabilization of FF is seen for thicknesses of 7 nm and 10 nm;
- A progressive improvement in FF is noted for FSF layers between 13 nm and 20 nm.

The reduction in fill factor for thinner layers is primarily due to the combined effect of decreasing output voltage and increasing series resistance within the cell. Thermal agitation, induced by the temperature rise in thin layers, increases resistivity, which deteriorates the internal transport conditions and lowers the FF.

Conversely, the improvement observed for thicker FSF layers is attributed to a decrease in effective resistivity, resulting from a reduction in bulk recombination. This leads to more efficient carrier extraction and an enhancement of the maximum power point.

4.3.Effect of Temperature on Open-Circuit Voltage (V_{oc})

Figure 6 illustrates the variation of open-circuit voltage (V_{oc}) in a heterojunction solar cell as a function of temperature, for various FSF layer thicknesses. The observed behavior is consistent with findings reported in previous studies **[2, 16, 17, 18].**

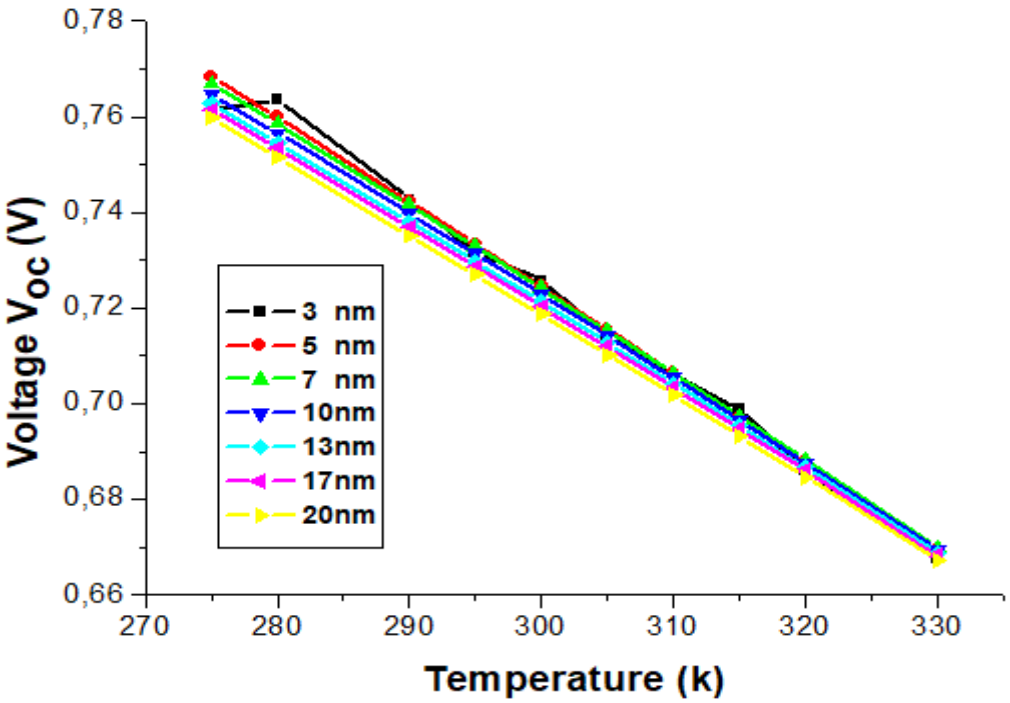

Figure 6 : Variation of Open-Circuit Voltage with Temperature for Different FSF Layer Thicknesses

The analysis of Figure 6 highlights the significant negative impact of temperature on the open-circuit voltage (V_{oc}). A linear decrease in V_{oc} is observed as temperature increases. This decline is attributed to the enhanced thermal agitation of atoms in the semiconductor material, which leads to an increase in the reverse saturation current (I_0).

According to Equation (3), I_0 which is linked to thermally activated charge carrier recombination rises rapidly with temperature. As described by Equation (6), this results in a steady decline in open-circuit voltage. These findings are consistent with previous theoretical and experimental studies, which report that the efficiency of photovoltaic cells decreases with rising temperature **[18, 19, 20, 21]**.

Thus, as the temperature increases, the open-circuit voltage of the solar cell decreases, leading consequently to a drop in energy conversion efficiency.

5. Conclusion

The influence of temperature on a heterojunction solar cell with the structure (p^+)-a-Si:H / (n)-c-Si / (n^+)-a-Si:H has been investigated using the Atlas simulator from the TCAD-SILVACO software suite. The study focused on photovoltaic cells with varying FSF layer thicknesses.

The results confirm a negative temperature effect on key performance parameters such as the open-circuit voltage (V_{oc}) and short-circuit current density (J_{sc}), particularly in cells with thin front layers. However, improvements in both efficiency and fill factor were observed for cells with a 20 nm FSF layer, suggesting better thermal stability in those configurations.

These findings emphasize the importance of considering local climatic conditions, especially temperature variations, when designing and optimizing heterojunction solar cells for real-world applications.

REFERENCES

[1] Priyanka Singh, N.M. Ravindra, "Temperature dependence of solar cell performance—an analysis" (2012), Solar Energy Materials & Solar Cells, SciVerse ScienceDirect, https://doi.org/10.1016/j.solmat.2012.02.019

[2] Mutlucan Bayat and Mehmet Özalp, "The Temperature Effect on Solar Photovoltaic Module Efficiency" (2016), Karabuk University, Turkey, Akademik Platform. https://www.academia.edu/71746400/The_Temperature_Effect_on_Solar_Photovoltaic_Module_Efficiency?nav_from=7180e0be-e5eb-4ece-a237-2758bf87b312

[3] SILVACO International, "User's manual for ATLAS, version 5.12.1."

[4] Nandhini K.M., Kumar C., Premkumar M., Bizuwork D., "Leveraging opposition-based learning for PV model parameter estimation using an exponential distribution optimization algorithm" (2024).

[5] Sébastien Thibert, "Study on front metallization of silicon photovoltaic cells," PhD thesis, University of Grenoble, 2006.

[6] Wen C., Fu C., Tang J.L., et al., "The influence of environmental temperatures on single crystalline and polycrystalline silicon solar cell performance" (2012), Science China-Physics, Mechanics & Astronomy, 55: 235–241. https://www.academia.edu/53323558/The_influence_of_environment_temperatures_on_single_crystalline_and_polycrystalline_silicon_solar_cell_performance?email_work_card=title

[7] Liao Z.L., Ruan X.B., "A new method on computing series resistance of silicon solar cells" (in Chinese), Trans. China Electrotech Soc., 2008.

[8] Mohsin A. Koondhar et al., "Temperature and irradiance-based analysis of PV module specific variation" (2020), Jurnal Teknologi, 83(6), 1–17. https://doi.org/10.11113/jurnalteknologi.v83.16609|

[9] Sidibba A., Ndiaye D., El Bah M., Bouhamady S., "Analytical modeling and determination of characteristic parameters of commercial PV technologies" (2018), Journal of Power and Energy Engineering, 6, 14–27. https://doi.org/10.4236/jpee.2018.63002

[10] Krustok J., Josepson R., Danilson M., et al., "Temperature dependence of $Cu2ZnSn(Se_xS_{1-x})_4$ monograin solar cells" (2010), Solar Energy Materials & Solar Cells.

[11] B.S.S. Ganesh Pardhu & Venkata Reddy Kota, "A novel AOA-based MPPT technique for 2S2P PV system under complex irradiations" (2025).

[12] Mohamed Saleck Heyine, "Performance analysis of a 50 MWc grid-connected PV plant in the SOMELEC network" (2023), PhD Thesis, University of Nouakchott.

[13] Bivour M. et al., "Influence of a-Si:H layer thickness on passivation quality in silicon heterojunction solar cells" (2012), Energy Procedia, 27, pp. 510–515. https://doi.org/10.1016/j.egypro.2012.07.098

[14] Taguchi M. et al., "High-efficiency hydrogenated amorphous silicon heterojunction solar cells" (1994), Japanese Journal of Applied Physics, 33(5B), pp. 3713–3719. https://doi.org/10.1143/JJAP.33.3713

[15] D.M. Fébba, R.M. Rubinger, A.F. Oliveira, E.C. Bortoni, "Impacts of temperature and irradiance on polycrystalline silicon solar cell parameters" (2018), Solar Energy.
https://www.academia.edu/94055837/Impacts_of_temperature_and_irradiance_on_polycrystalline_silicon_solar_cells_parameters?nav_from=878cd091-20fb-43f4-bd11-3171c81bb8ba

[16] F. Ghani, G. Rosengarten, M. Duke, J.K. Carson, "On the influence of temperature on crystalline silicon solar cell characterization parameters" (2015).
https://www.academia.edu/23720786/On_the_influence_of_temperature_on_crystalline_silicon_solar_cell_characterisation_parameters?email_work_card=view-paper

[17] Abhishek Sharan, B. Prasad, S. Chandril, "Study of temperature on performance of c-Si homo junction and a-Si/c-Si hetero junction solar cells" (2013), Int. J. Renewable Energy Research.
https://www.academia.edu/26882926/Study_of_temperature_on_performance_of_c_Si_homo_junction_and_a_Si_c_Si_hetero_junction_solar_cells?nav_from=d178cce8-f675-497b-8ed8-47c339993a9f

[18] P. Otero, J.A. Rodríguez, M. Vetter et al., "Simulation of the temperature dependence of a-Si:H solar cell current-voltage characteristics" (2011), 8th Spanish Conference on Electron Devices (CDE 2011).
https://www.academia.edu/87091757/Effect_of_High_Temperature_on_the_Efficiency_of_Grid_Connected_PV_System?nav_from=2112af59-b37f-492e-82f4-878d8ce83984

[19] Min-Jung Wu, Erik J. Timpson, Steve E. Watkins, "Temperature considerations in solar arrays" (2004), University of Missouri-Rolla.

[20] Abdulaziz Alkuhayli, Ahmed Telba, "Effect of high temperature on the efficiency of a grid-connected PV system" (2021), World Congress on Engineering.
https://www.academia.edu/87091757/Effect_of_High_Temperature_on_the_Efficiency_of_Grid_Connected_PV_System?nav_from=2112af59-b37f-492e-82f4-878d8ce83984

[21] R. Aliev, M. Abduvohidov, J. Gulomov, "Simulation of temperature influence on photoelectric properties of silicon solar cells" (2020), Physics Astronomy International Journal.

https://www.academia.edu/74591339/Simulation_of_temperatures_influence_to_photoelectric_properties_of_silicon_solar_cells?email_work_card=view-paper